Viscoelastic response of the impact process on dense suspensions

*Pradipto and Hayakawa, Phys. Fluids **33**, 093310 (2021)*

Pradipto and Hisao Hayakawa
Yukawa Institute for Theoretical Physics
Kyoto University

Kakenhi meeting, YITP
12/3/2021

Introduction

Suspensions

Mixture of macroscopic, undissolved particles in fluid

Solutions

water + salt solutions

Colloids

milk

- **DLVO Theory**
- **Thermal agitation**
- **Brownian motion**

Suspensions

cornstarch + water

- **Mechanical agitation**
- **Brownian motion is negligible**

+

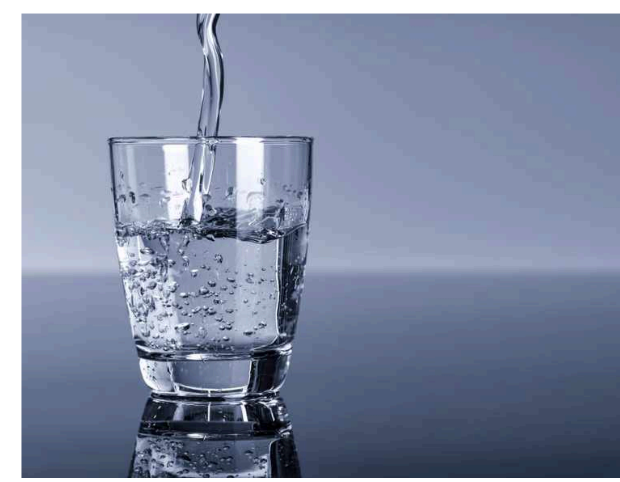

$< 1nm$ $\quad 1nm - 1\mu m$ $\quad 1\mu m - 100\mu m$

particle radius a

Our focus is on the simplest type of suspension: hard, athermal, non-attractive particles, suspended in a Newtonian fluid.

Introduction

Suspensions

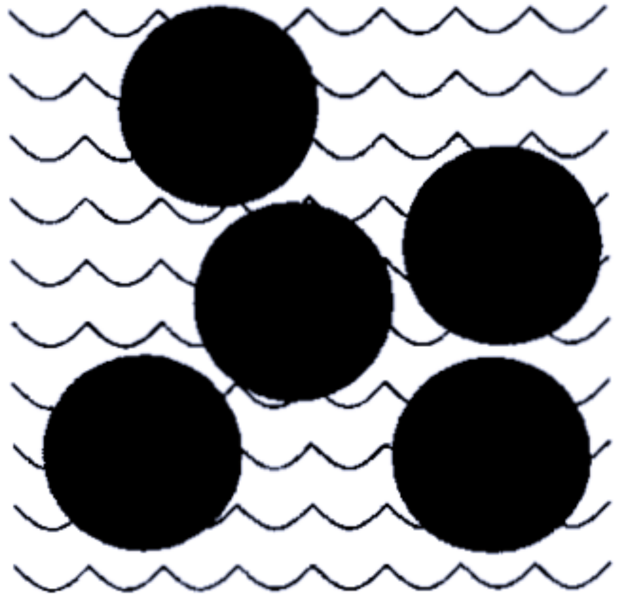

Flow speed

Length scale

$$Re = \frac{uL}{\nu}$$

Kinematic Viscosity

Low Reynolds number

$$Re \ll 1$$

Discontinuous shear thickening (DST) under shear

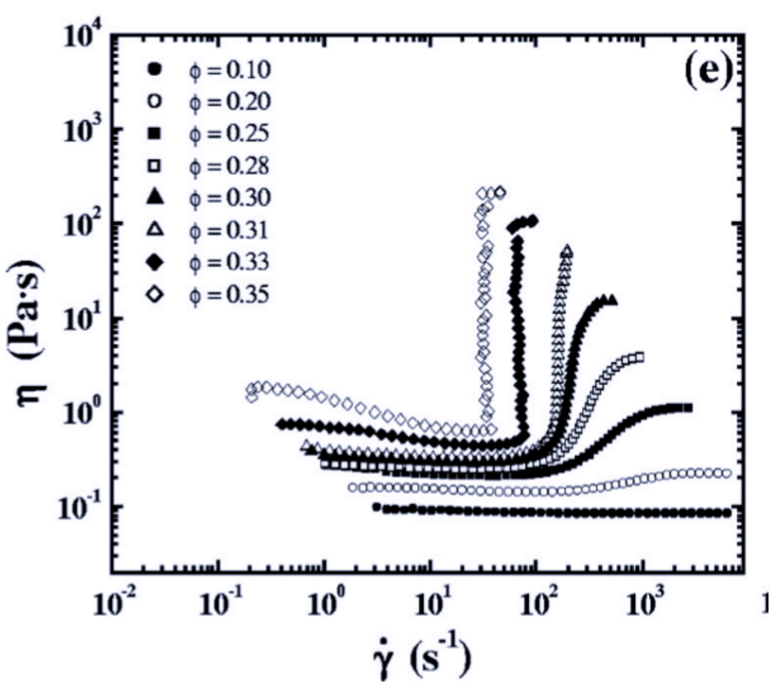

Stokes equation

$$\nabla p = \eta \nabla^2 \mathbf{u}$$

$$\nabla \cdot \mathbf{u} = 0$$

Egres and Wagner, J. Rheol **49**, 719-746 (2005)

Introduction Dense suspensions under impact

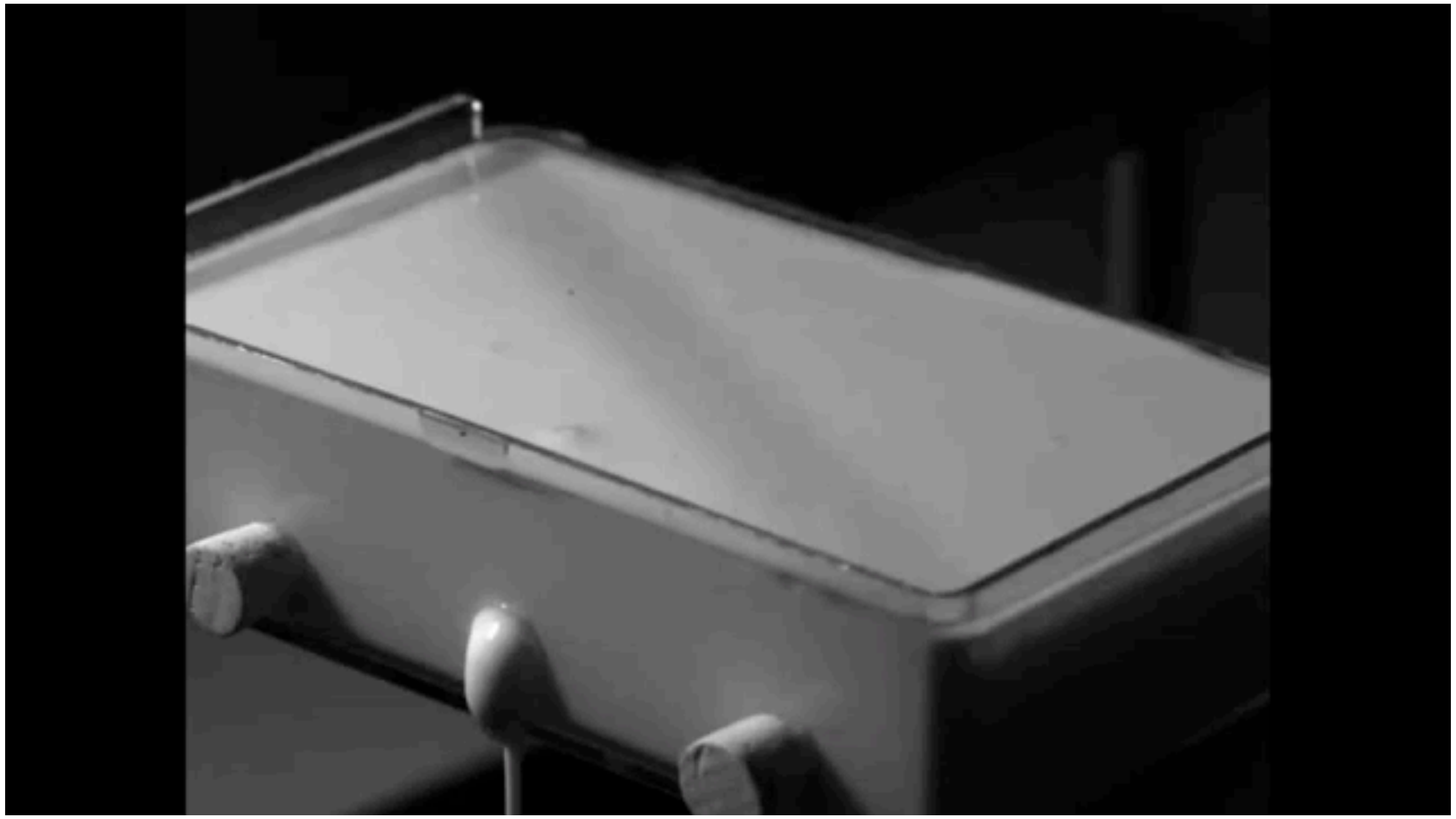

source: https://www.youtube.com/watch?v=hP88C-_LgnE&list=PLVjiIPzFTOLpxiwdwrFuPYSIBpr6jFm32

Impact-induced hardening

Occurs on the simplest type of suspensions

Cannot be observed in liquid or particles alone

Physical explanations remain elusive

- Inherently far-from-equilibrium
- Highly dissipative —> transient

Impact-induced hardening

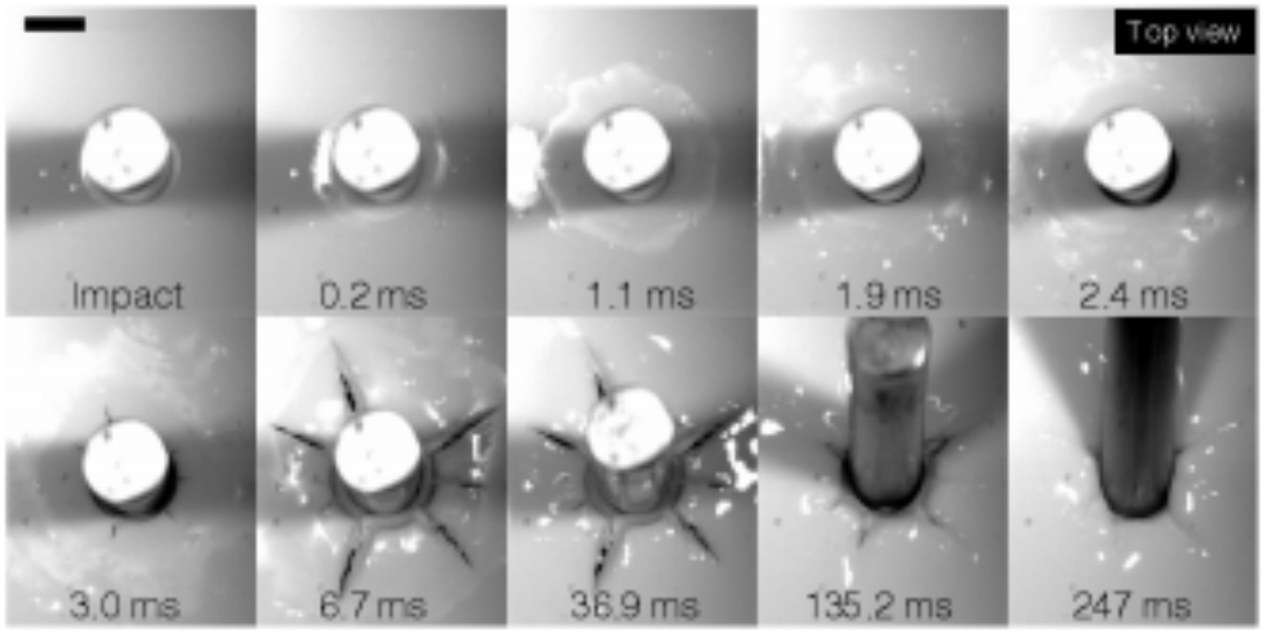

Even fracture can exist!

Roche et al, PRL 2013

Run on suspension

Brown, et. al., Rep. Prog. Phys 77, 046602 (2014).

Liquid body armor

https://www.youtube.com/watch?v=L5Ts9lYZIDk

Introduction Dense suspensions under impact

Elastic rebound

Egawa and Katsuragi, Phys. Fluids **31**, 053304 (2019)

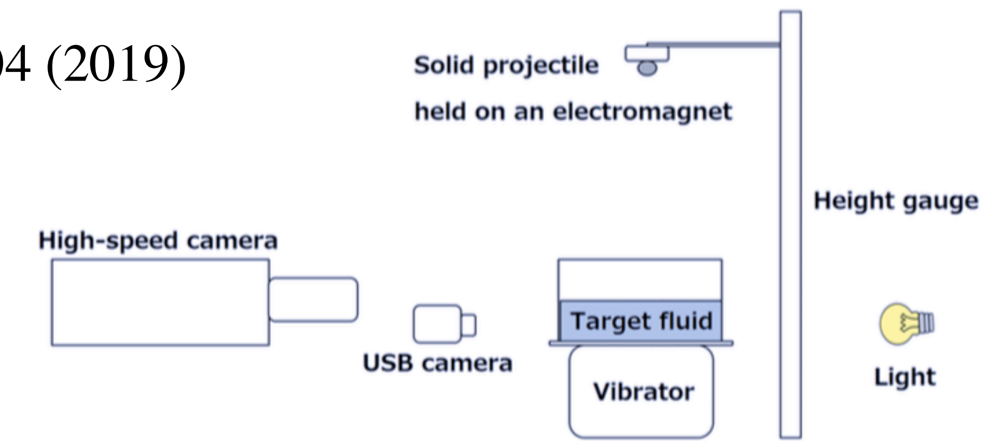

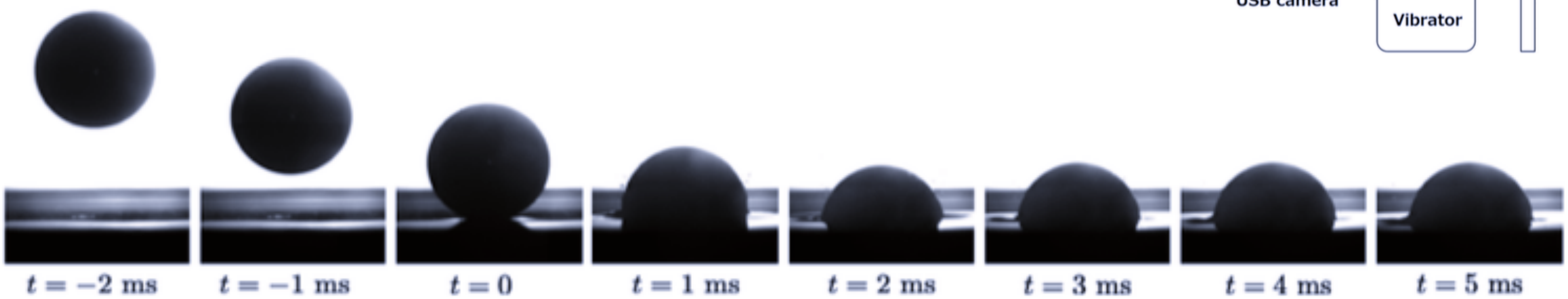

Experiment

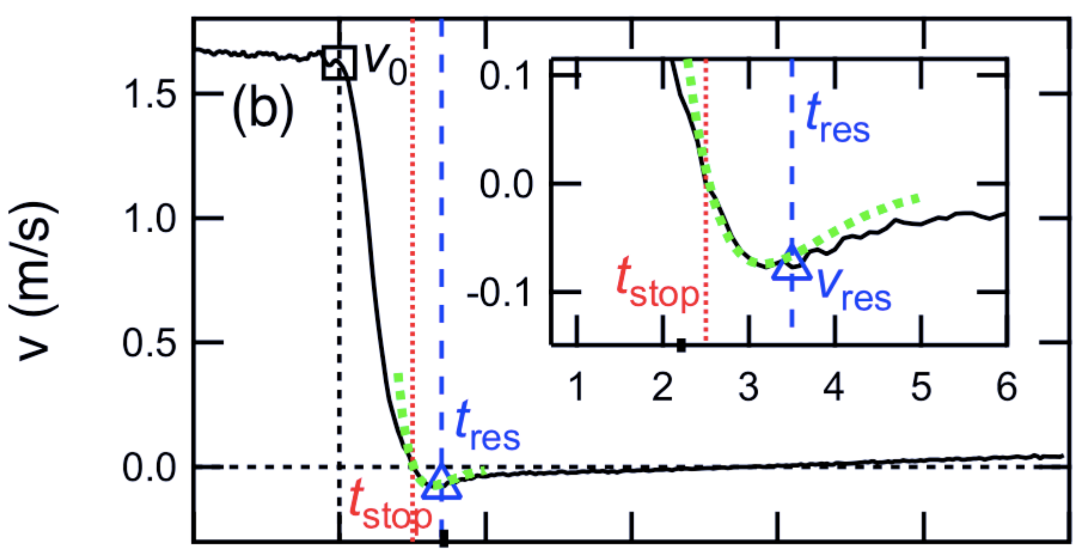

Simulation

Pradipto and Hayakawa, Phys. Rev. Fluids **6**, 033301 (2021).

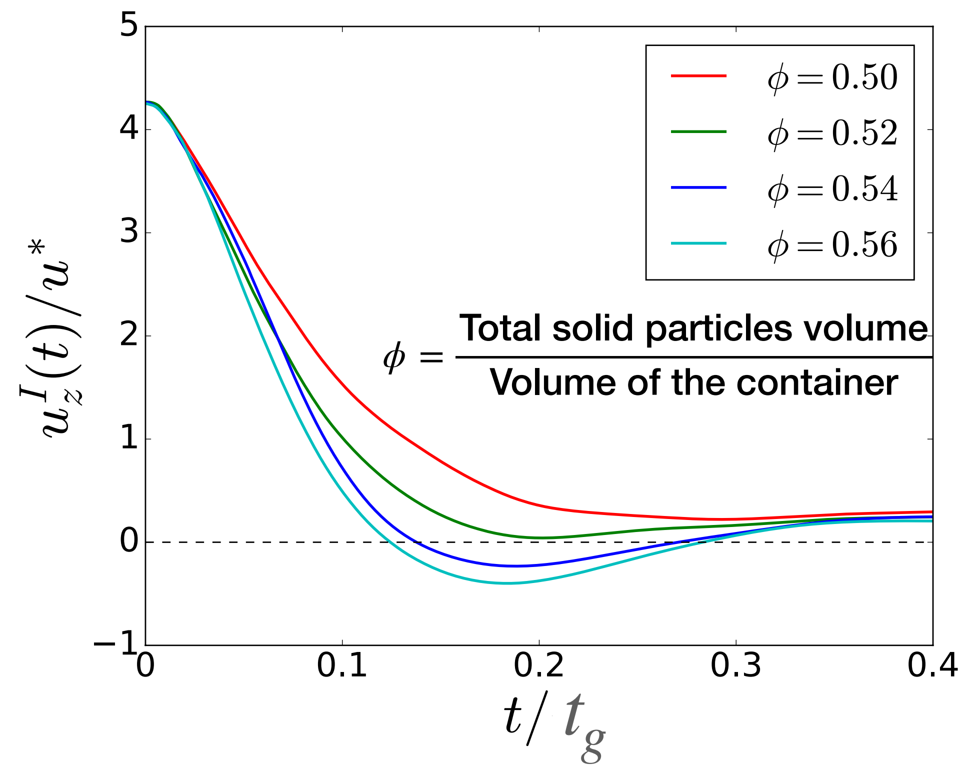

Different from shear jamming and shear thickening

Pradipto and Hayakawa, Phys. Rev. Fluids **6**, 033301 (2021).

Normal stress

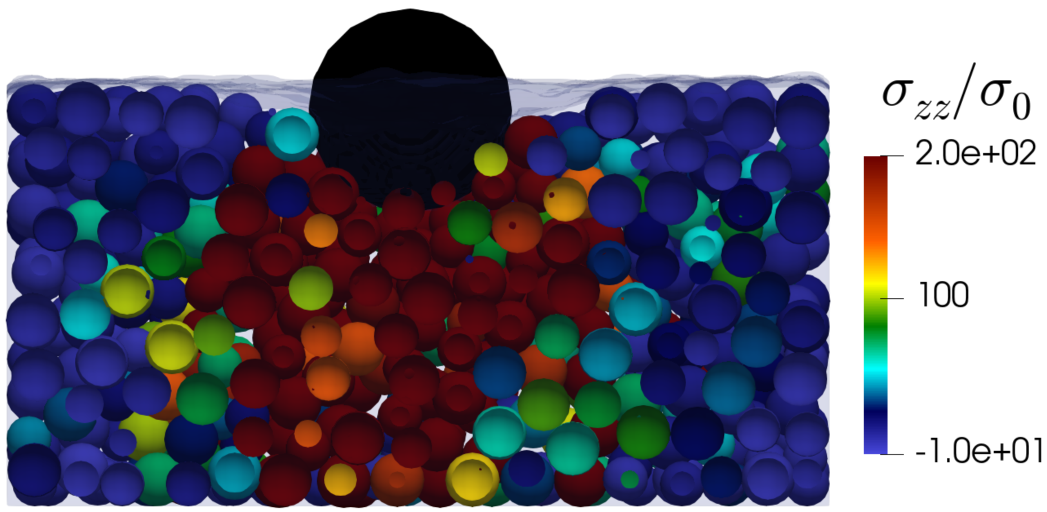

Shear stress

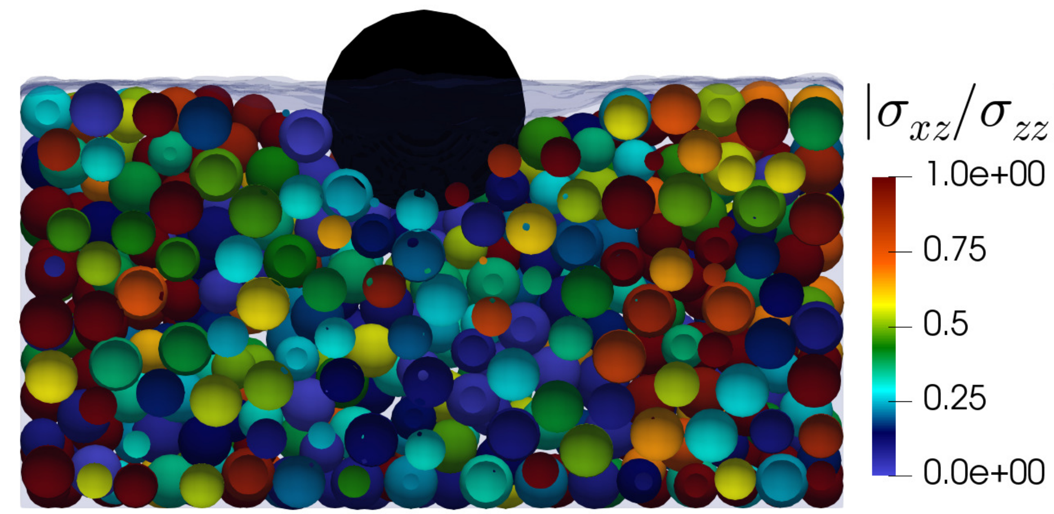

Experimentally observed

Waitukaitis and Jaeger, Nature **487**, 205 (2012)

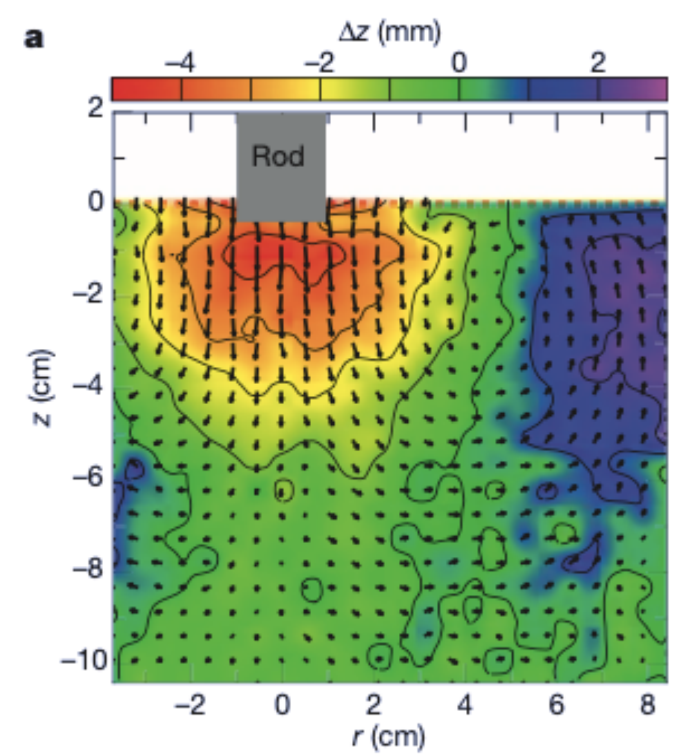

Dynamically jammed region

- Localized and transient jammed area beneath the impactor
- High normal stress instead of shear stress

Rebound depends on impact velocity and frictional interactions between particles

Pradipto and Hayakawa, Phys. Rev. Fluids **6**, 033301 (2021).

Rebounds also depend on the impact velocity ..

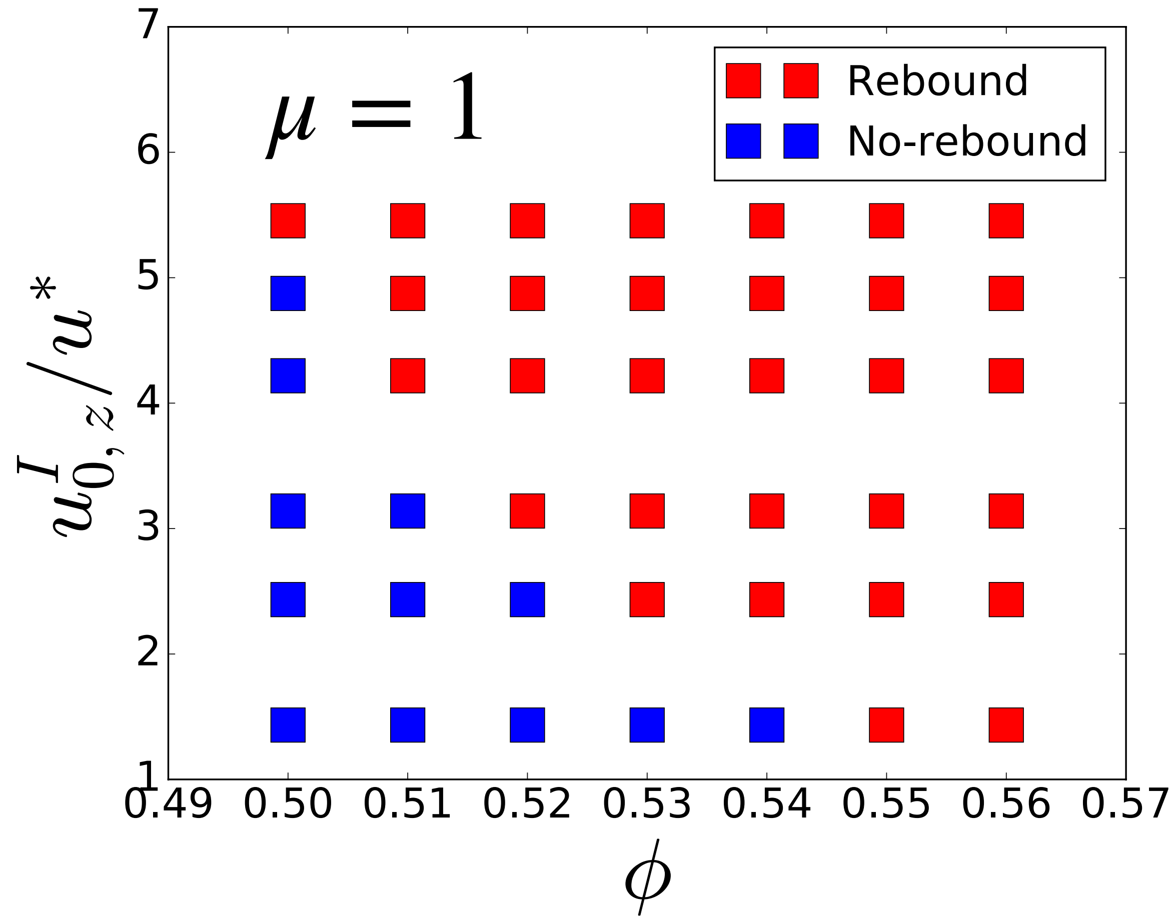

We can run on top suspension but we'll sink if we walk

.. and friction coefficients

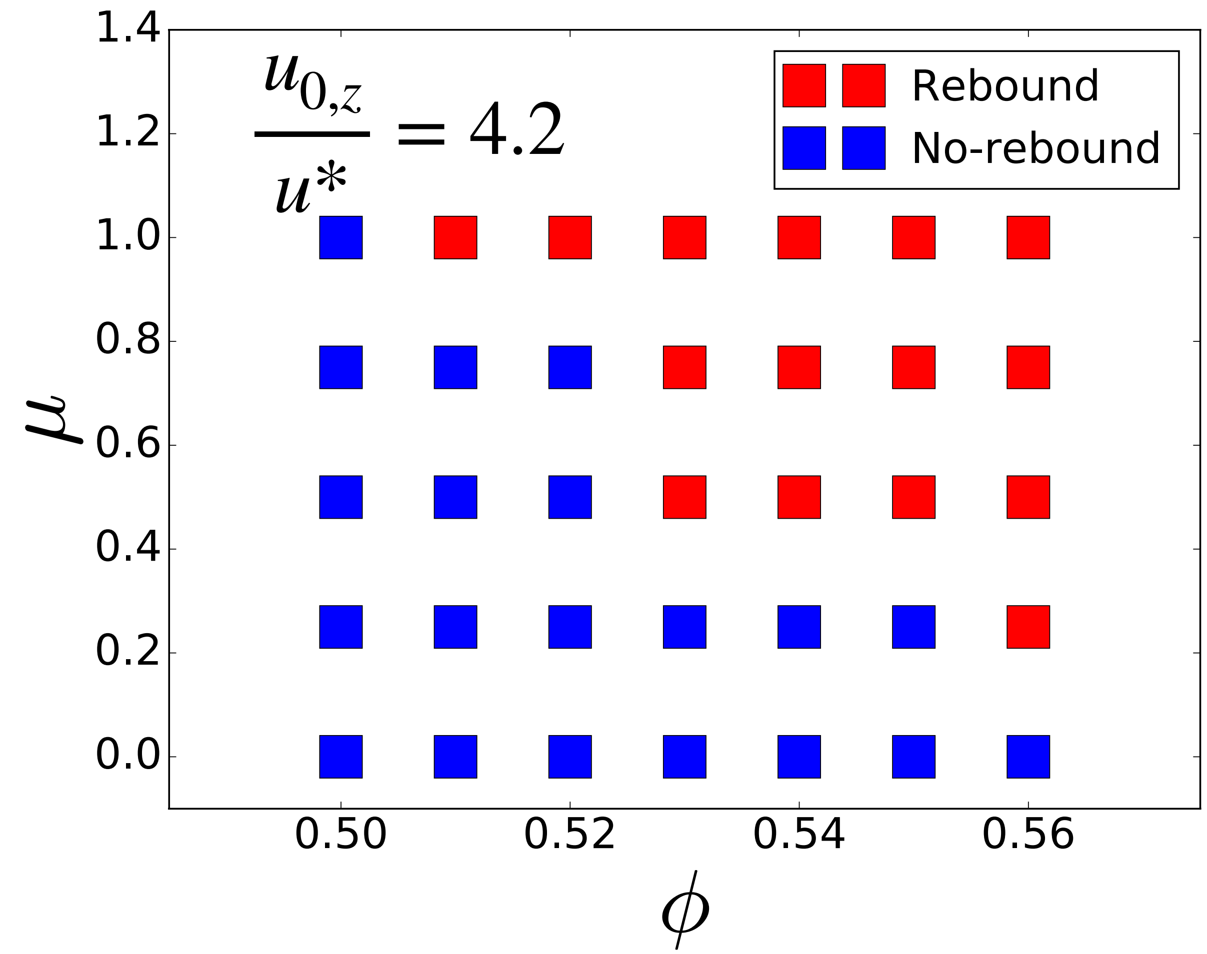

Frictional interaction increases the contact duration between particles that leads to a stronger hardening

Power-law relations between u_0, $F_{\max}$, and $t_{\max}$

Brassard, et. al, JFM **923**, A38 (2021)

Experiment

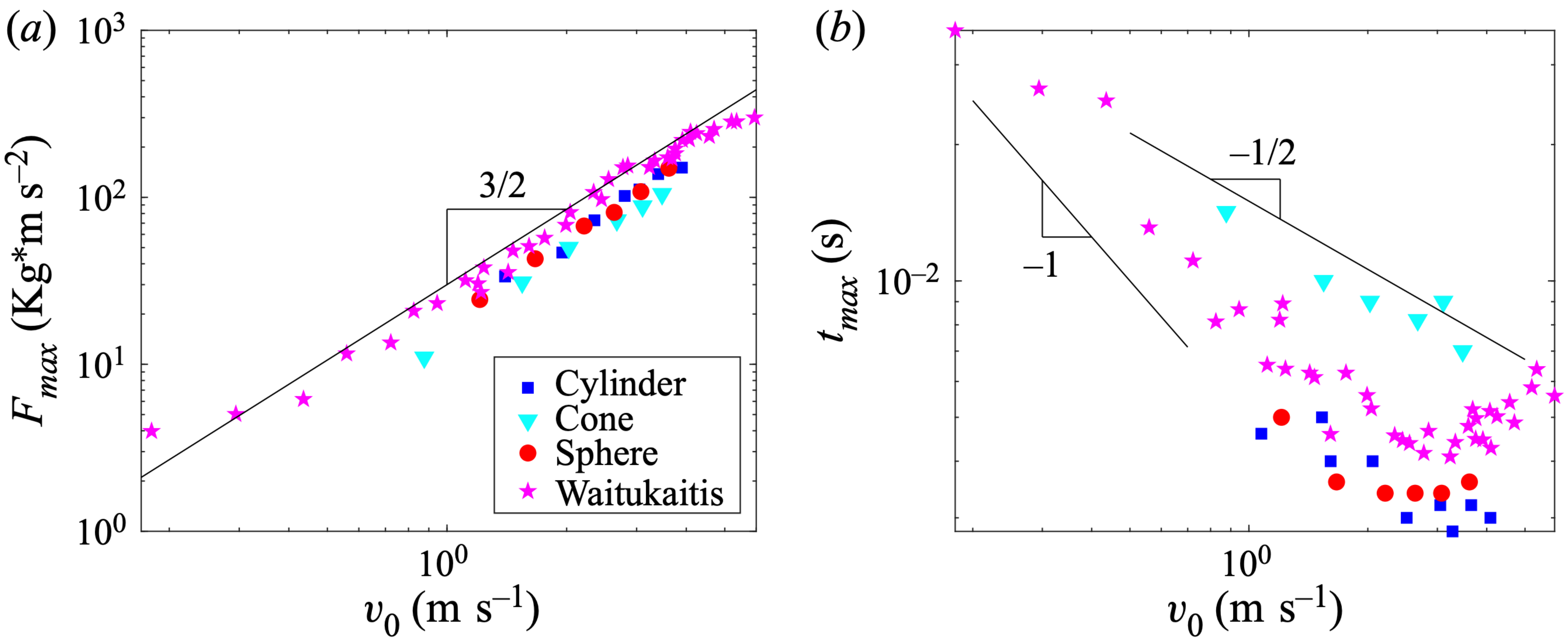

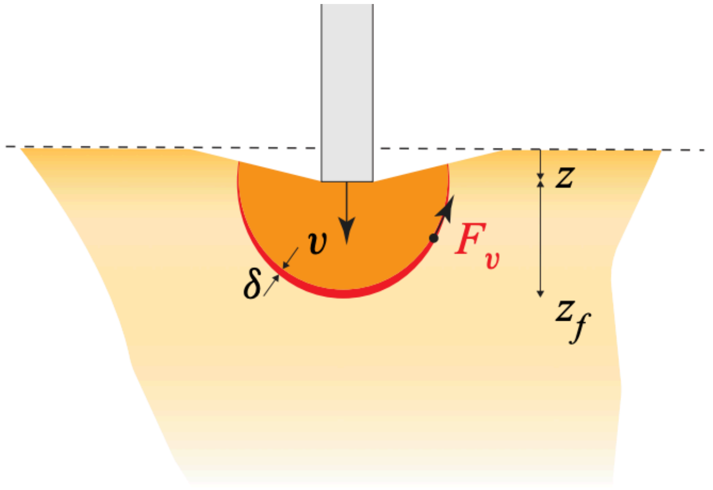

Viscous force from the dynamically jammed region

$$F_v = -C_v \pi D \eta_s k z \frac{v}{\delta}.$$

Cannot recover the elastic rebound

Is there any connection between this power-law relation and the rebound motion?

Ingredients of our simulation

Hydrodynamic Interaction

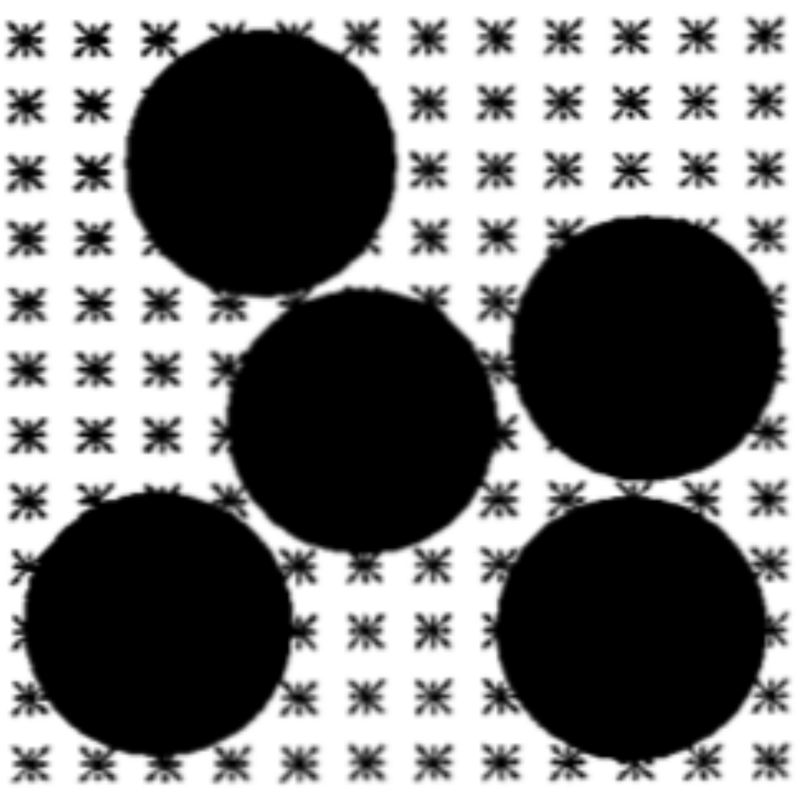

Contact between particles

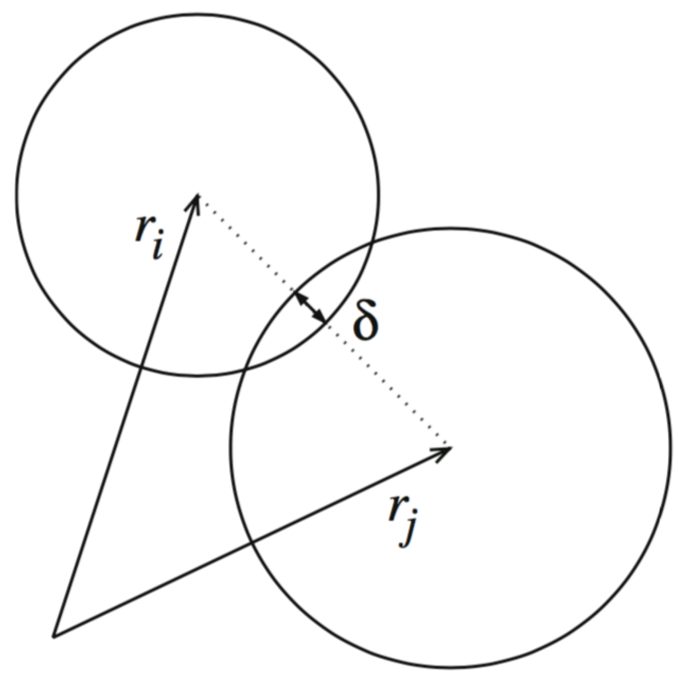

Free surface of the liquid

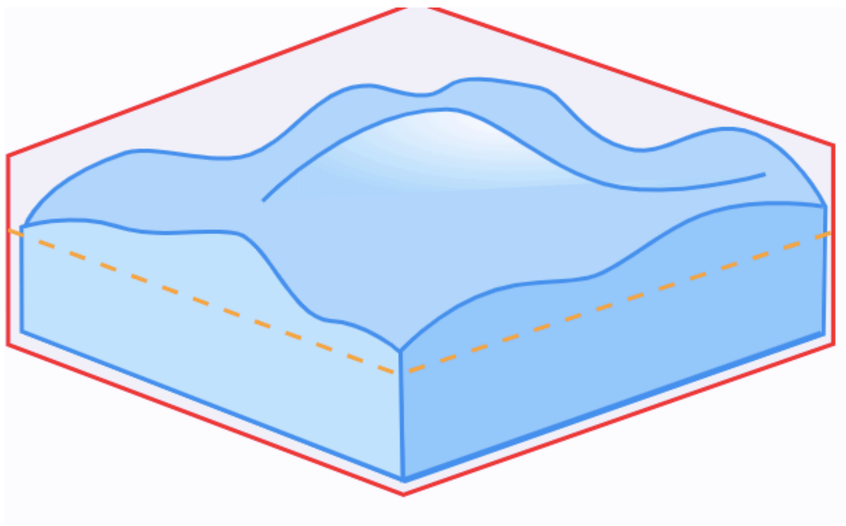

Hydrodynamic interactions: LBM + *Lubrication corrections*

LBM

Underestimate hydrodynamic force on small gap due to shared nodes

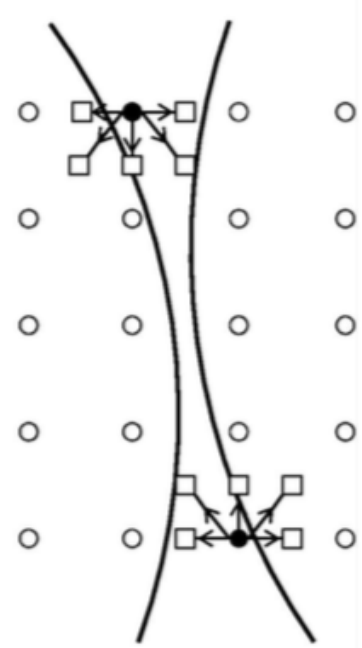

- Calculate hydrodynamic field on nodes from f_i

  $f_i \rightarrow$ lattice distribution function

- Calculate hydrodynamic force on the particles

Lubrication corrections

Nguyen and Ladd, PRE **66**, 046708,(2002)

Corrections 2-body resistance matrix

$$\begin{pmatrix} \mathbf{F}_1 \\ \mathbf{T}_1 \\ \mathbf{T}_2 \\ \mathbf{S}_1 \\ \mathbf{S}_2 \end{pmatrix} = - \begin{pmatrix} \mathbf{A}_{11} & -\mathbf{B}_{11} & \mathbf{B}_{22} \\ \mathbf{B}_{11} & \mathbf{C}_{11} & \mathbf{C}_{12} \\ -\mathbf{B}_{22} & \mathbf{C}_{12} & \mathbf{C}_{22} \\ \mathbf{G}_{11} & \mathbf{H}_{11} & \mathbf{H}_{12} \\ \mathbf{G}_{22} & -\mathbf{H}_{21} & \mathbf{H}_{22} \end{pmatrix} \begin{pmatrix} \mathbf{U}_{12} \\ \boldsymbol{\Omega}_1 \\ \boldsymbol{\Omega}_2 \end{pmatrix}$$

With $\mathbf{U}_{12} = \mathbf{U}_2 - \mathbf{U}_1$ and $\mathbf{F}_2 = -\mathbf{F}_1$

- No external or local flow field contributions
- Only activated when the gap is small
- Submatrices are calculated with leading order coefficients in *Kim and Karilla, Microhydrodynamics (1991)*

c.f. The actual 2-body resistance matrix

Jeffrey and Ohnishi, JFM, (1984)

Jeffrey, Phys. Fluids, (1992)

Ichiki, et. al, arXiv:1302.0461

$$\begin{bmatrix} \boldsymbol{F}^{(1)} \\ \boldsymbol{F}^{(2)} \\ \boldsymbol{T}^{(1)} \\ \boldsymbol{T}^{(2)} \\ \boldsymbol{S}^{(1)} \\ \boldsymbol{S}^{(2)} \end{bmatrix} = - \begin{bmatrix} \mathsf{A}_{11} & \mathsf{A}_{12} & \widetilde{\mathsf{B}}_{11} & \widetilde{\mathsf{B}}_{12} & \widetilde{\mathsf{G}}_{11} & \widetilde{\mathsf{G}}_{12} \\ \mathsf{A}_{21} & \mathsf{A}_{22} & \widetilde{\mathsf{B}}_{21} & \widetilde{\mathsf{B}}_{22} & \widetilde{\mathsf{G}}_{21} & \widetilde{\mathsf{G}}_{22} \\ \mathsf{B}_{11} & \mathsf{B}_{12} & \mathsf{C}_{11} & \mathsf{C}_{12} & \widetilde{\mathsf{H}}_{11} & \widetilde{\mathsf{H}}_{12} \\ \mathsf{B}_{21} & \mathsf{B}_{22} & \mathsf{C}_{21} & \mathsf{C}_{22} & \widetilde{\mathsf{H}}_{21} & \widetilde{\mathsf{H}}_{22} \\ \mathsf{G}_{11} & \mathsf{G}_{12} & \mathsf{H}_{11} & \mathsf{H}_{12} & \mathsf{M}_{11} & \mathsf{M}_{12} \\ \mathsf{G}_{21} & \mathsf{G}_{22} & \mathsf{H}_{21} & \mathsf{H}_{22} & \mathsf{M}_{21} & \mathsf{M}_{22} \end{bmatrix} \cdot \begin{bmatrix} \boldsymbol{U}^{(1)} - \boldsymbol{u}^{\infty}(\boldsymbol{x}_1) \\ \boldsymbol{U}^{(2)} - \boldsymbol{u}^{\infty}(\boldsymbol{x}_2) \\ \boldsymbol{\Omega}^{(1)} - \boldsymbol{\Omega}^{\infty} \\ \boldsymbol{\Omega}^{(2)} - \boldsymbol{\Omega}^{\infty} \\ \boldsymbol{E}^{(1)} - \boldsymbol{E}^{\infty} \\ \boldsymbol{E}^{(2)} - \boldsymbol{E}^{\infty} \end{bmatrix}$$

Hydrodynamic interactions: Benchmark tests

1. Two particles under simple shear

Theory

Jeffrey and Ohnishi, JFM, (1984)
Jeffrey, Phys. Fluids, (1992)
Ichiki, et. al, arXiv:1302.0461

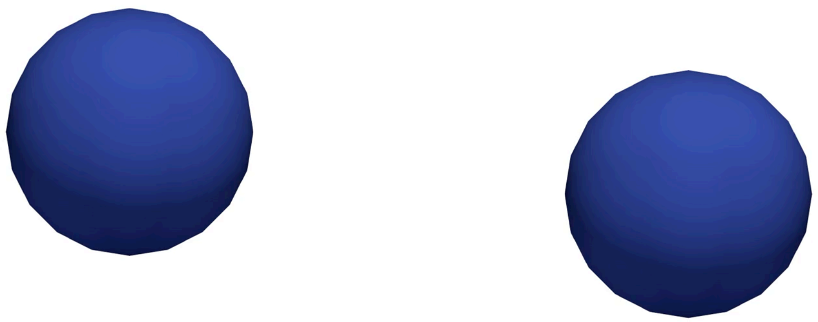

Particles don’t make contact

LBM+Lubrication corrections

Particles don’t make contact

LBM Only

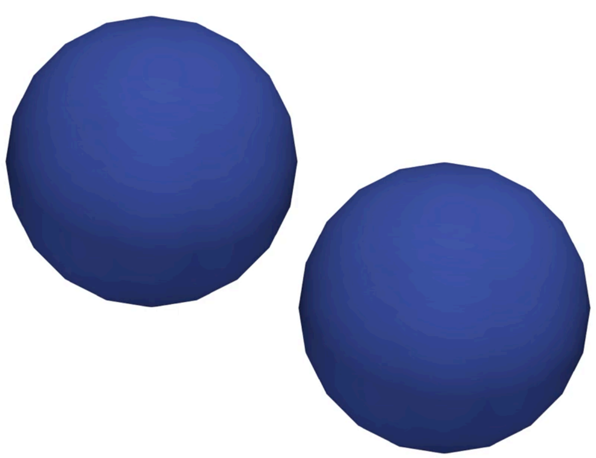

Particles make contact

Free surface - Mass tracking algorithm

Leonardi, et al., Phys. Rev. E **92,** 052204 (2015)

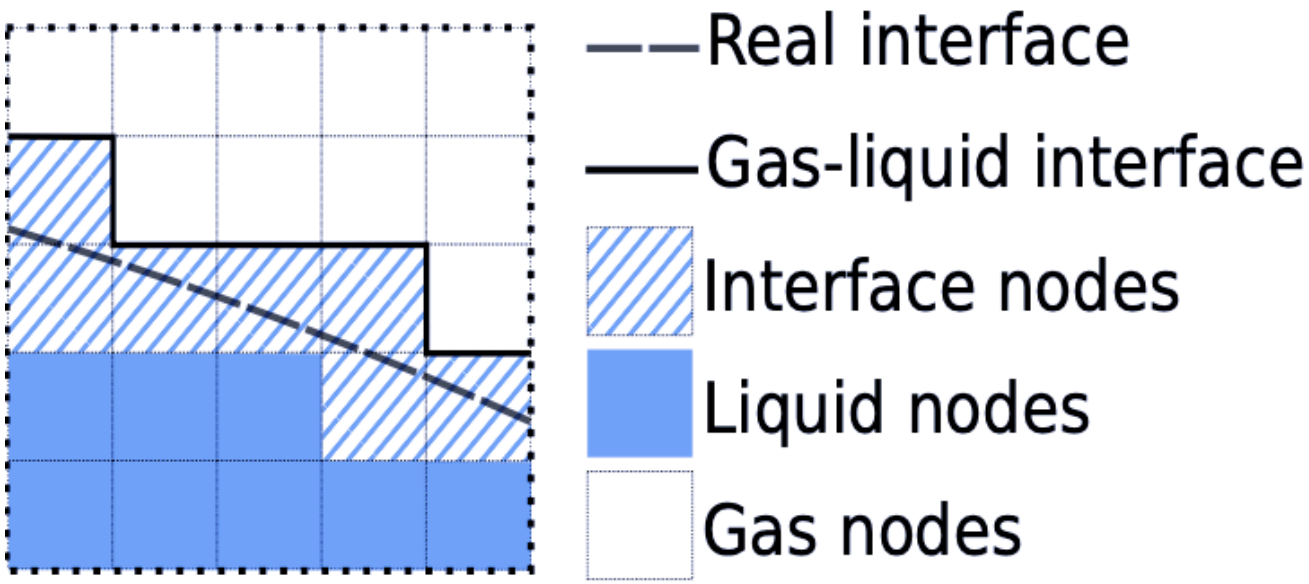

$$m_f(\mathbf{r}, t) = \lambda \rho_f(\mathbf{r}, t)$$

Liquid fraction $\begin{cases} \lambda = 1 & \text{if the node is liquid} \\ 0 < \lambda < 1 & \text{if the node is interface,} \\ \lambda = 0 & \text{if the node is gas.} \end{cases}$

α_i depends on the neighbors

$$\alpha_i = \begin{cases} \frac{1}{2}[\lambda(\mathbf{r}, t) + \lambda(\mathbf{r} + \mathbf{c}_{i'}, t)] & \text{if neighbor is interface} \\ 1 & \text{if neighbor is fluid} \\ 0 & \text{if neighbor is gas} \end{cases}$$

Evolution equation

$$m_f(t + \Delta t) = m_f(t) + \sum_i \alpha_i (f_{i'}(\mathbf{r} + \mathbf{c}_{i'}, t) - f_i(\mathbf{r}, t)),$$

$$m_f(\mathbf{x}, t) = 0$$

⇩

Transform interface to gas

⇩

Liquid neighbors become interface

$$m_f(\mathbf{x}, t) = \rho_f^*(\mathbf{x}, t)$$

⇩

Transform interface to liquid

⇩

Gas neighbors become interface

Contact between suspended particles

Luding. S, Granular Matter, 2008, **10**, 235

Normal part

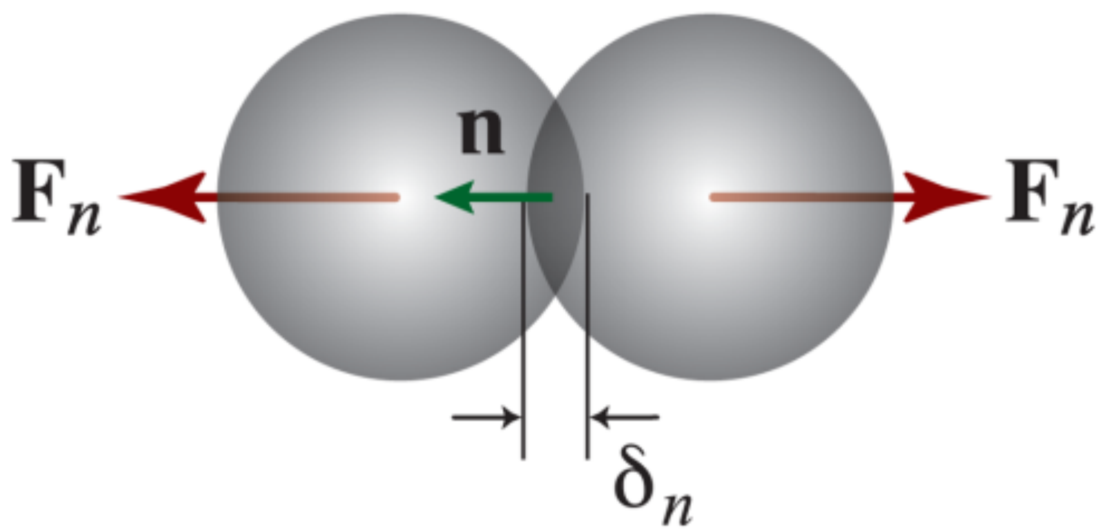

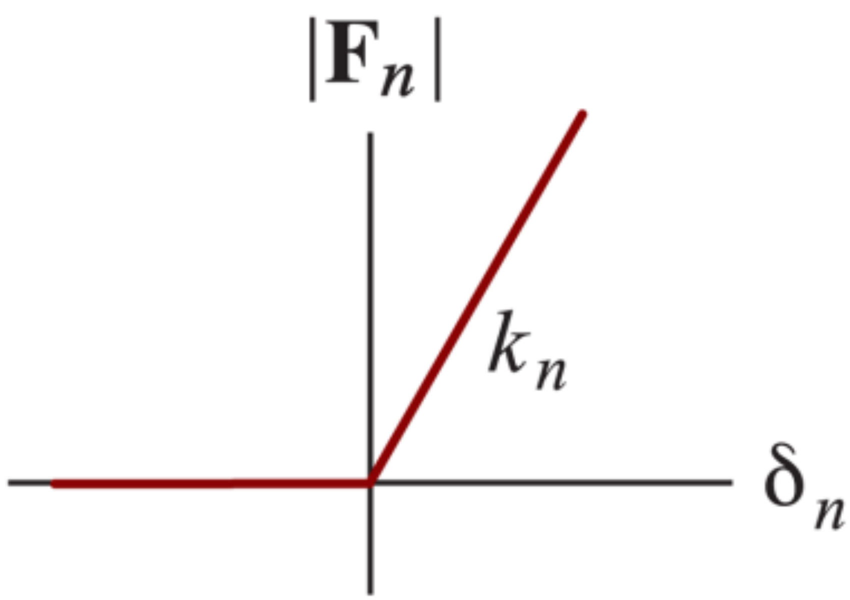

Tangential part

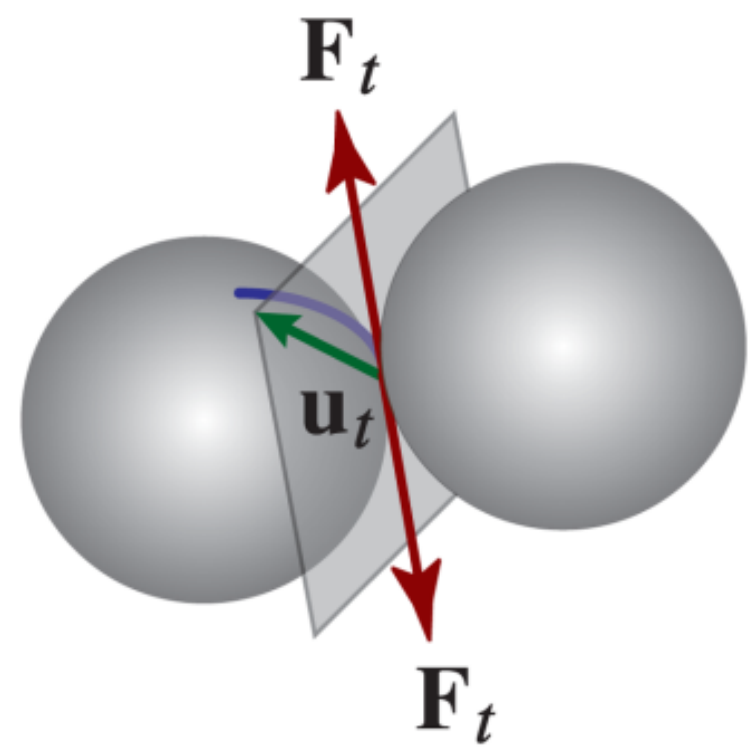

Coulomb friction

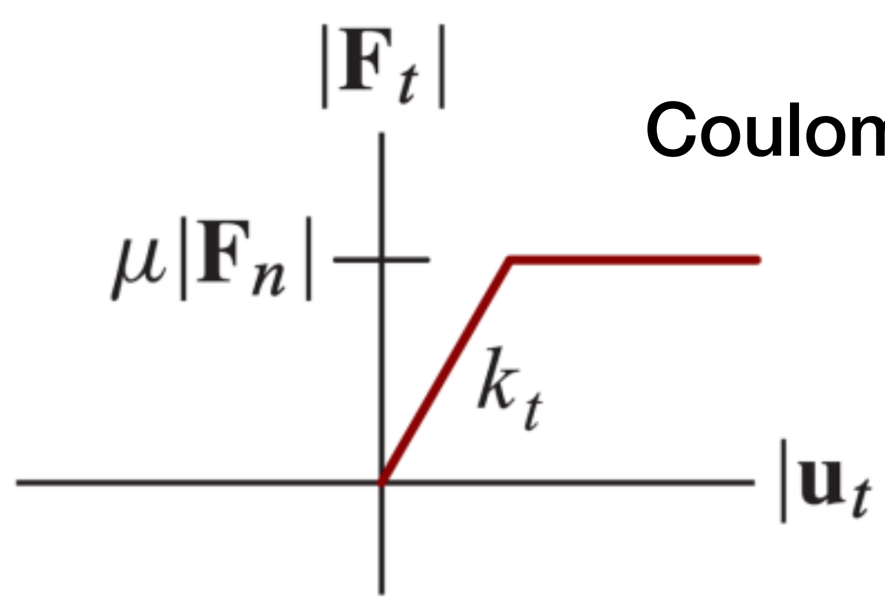

Simulation setup

Egawa and Katsuragi, Phys. Fluids **31**, 053304 (2019)
Pradipto and Hayakawa, Phys. Rev. Fluids **6**, 033301 (2021).

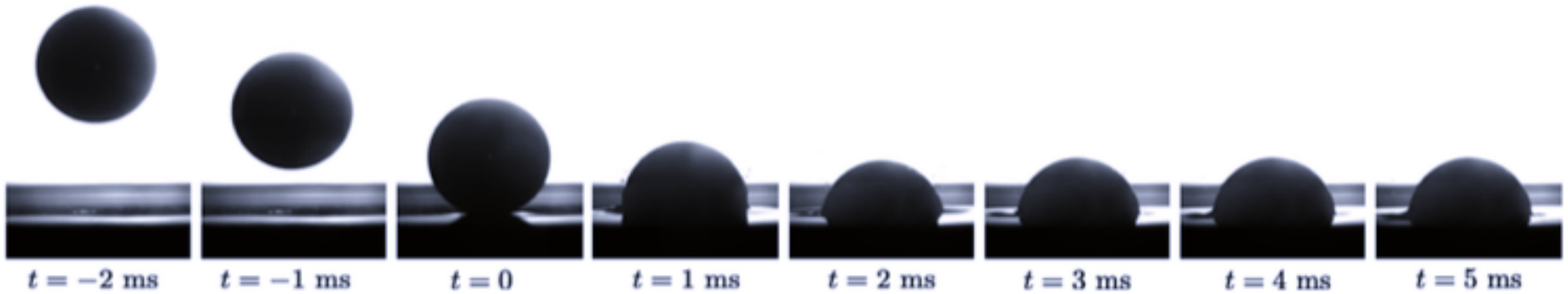

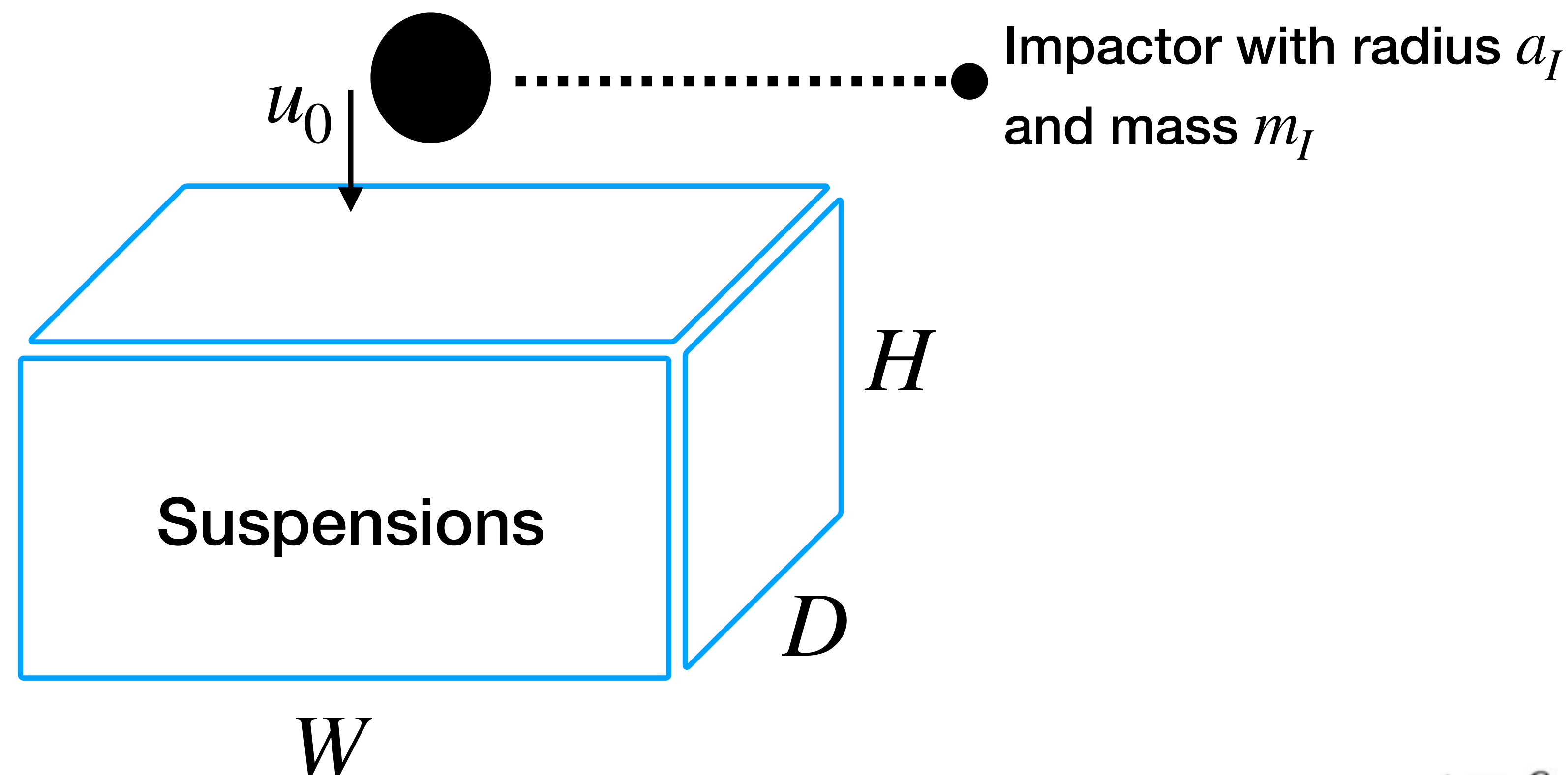

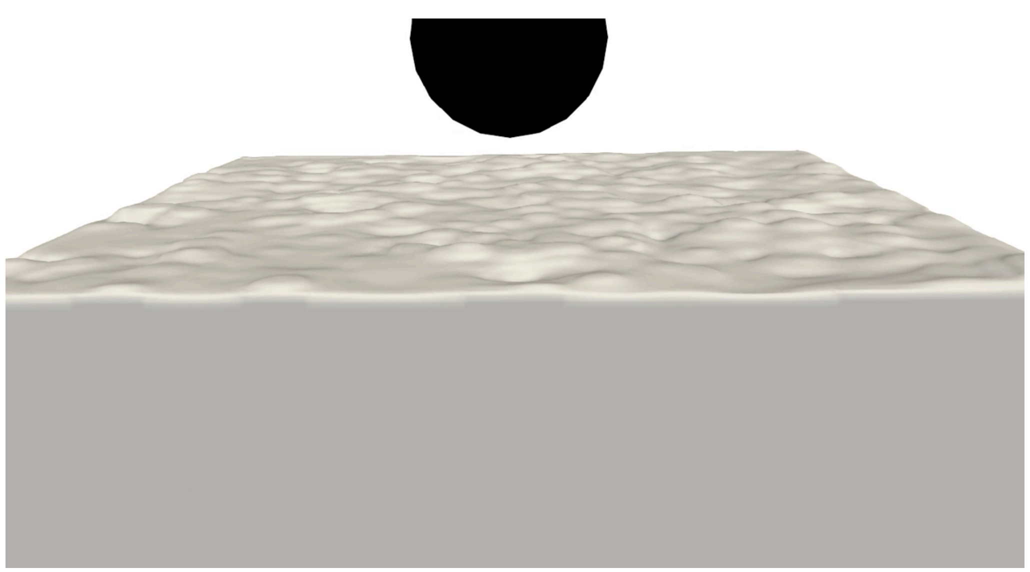

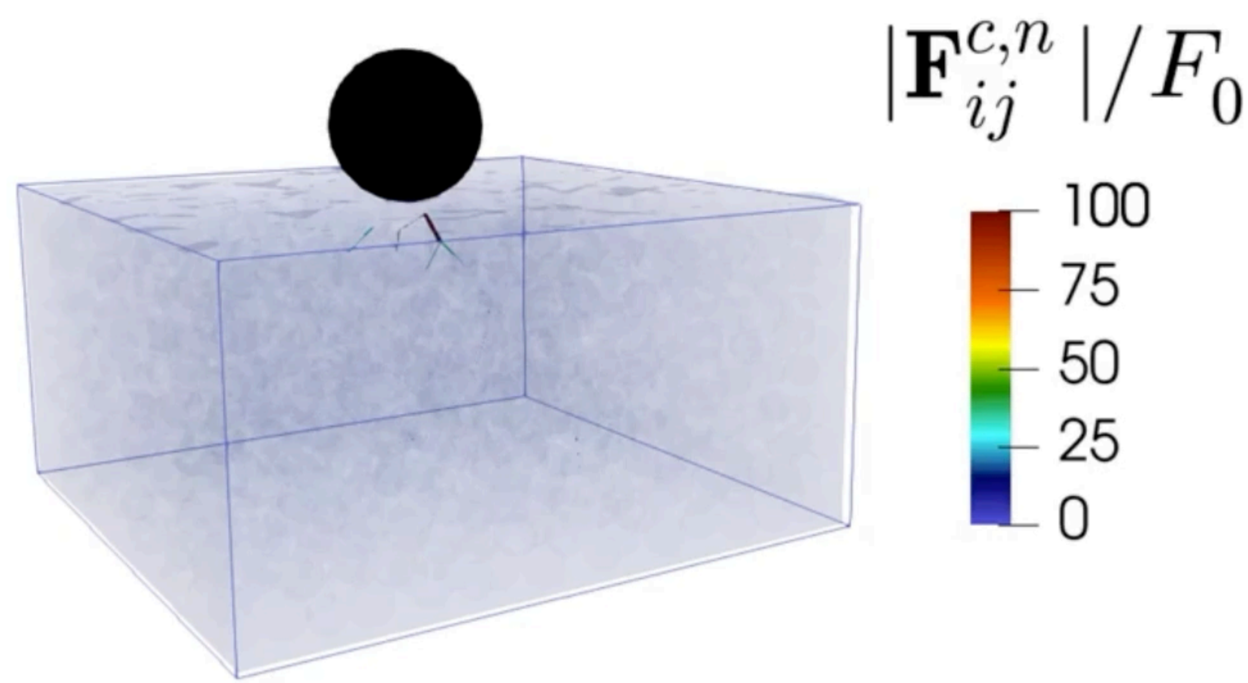

Maximum force exerted on the impactor ($F_{\max}$) and time to reach it ($t_{\max}$)

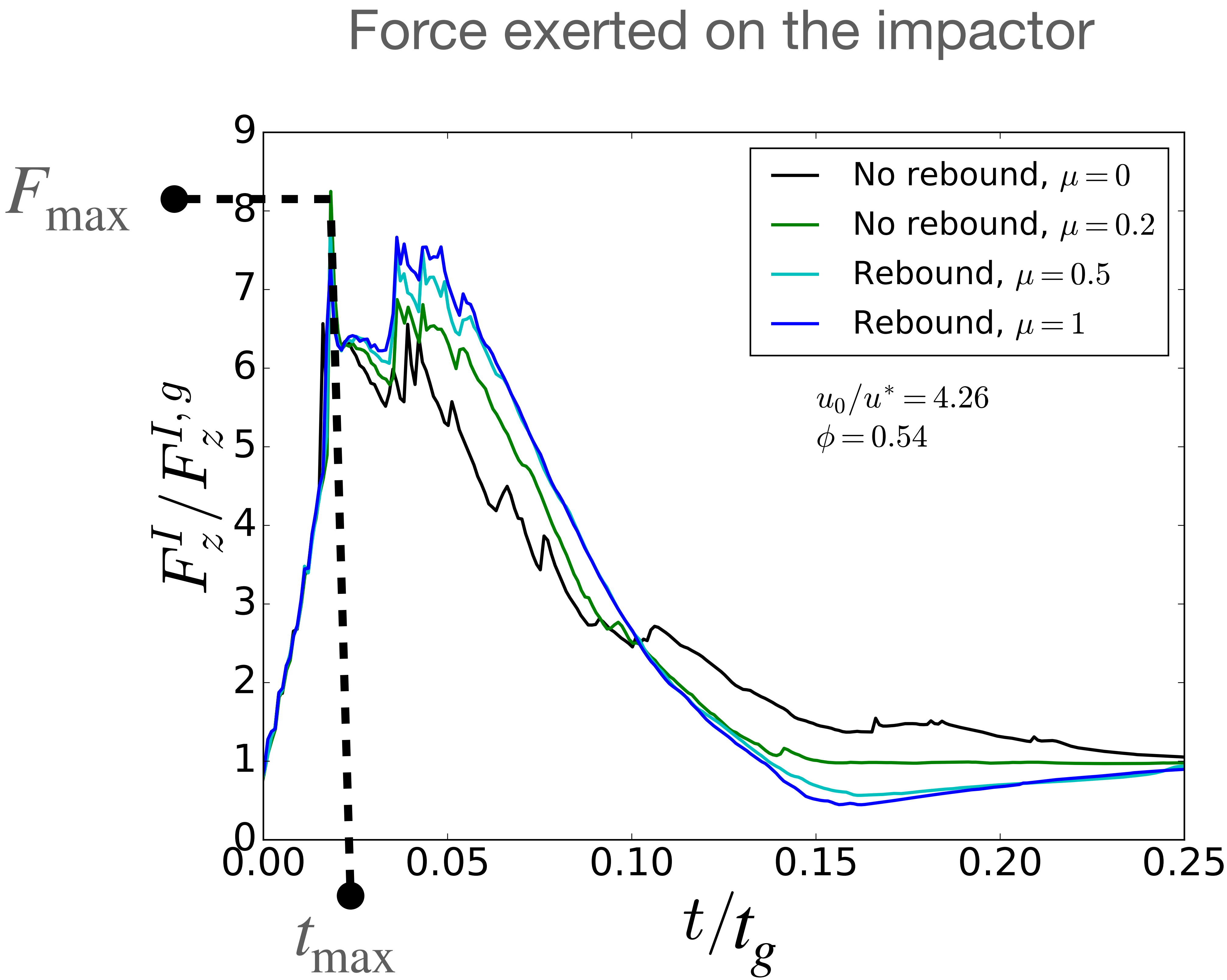

Crossover and power-law relationship between $F_{\max}$ and u_0

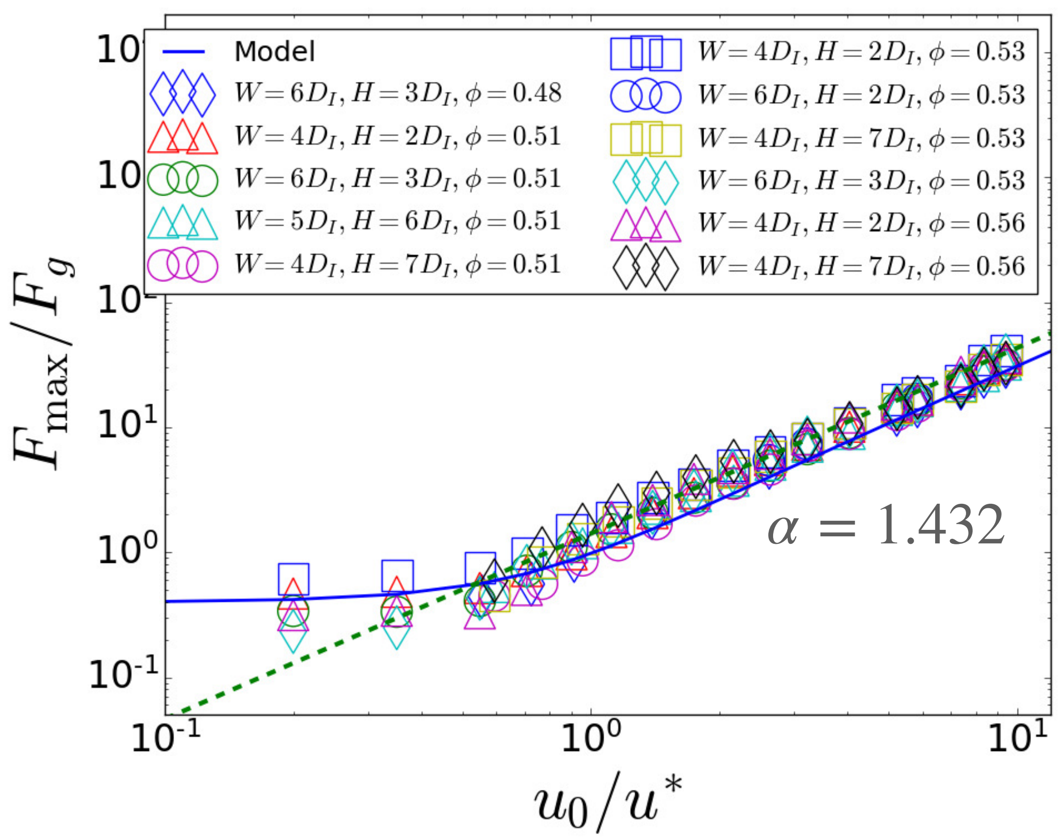

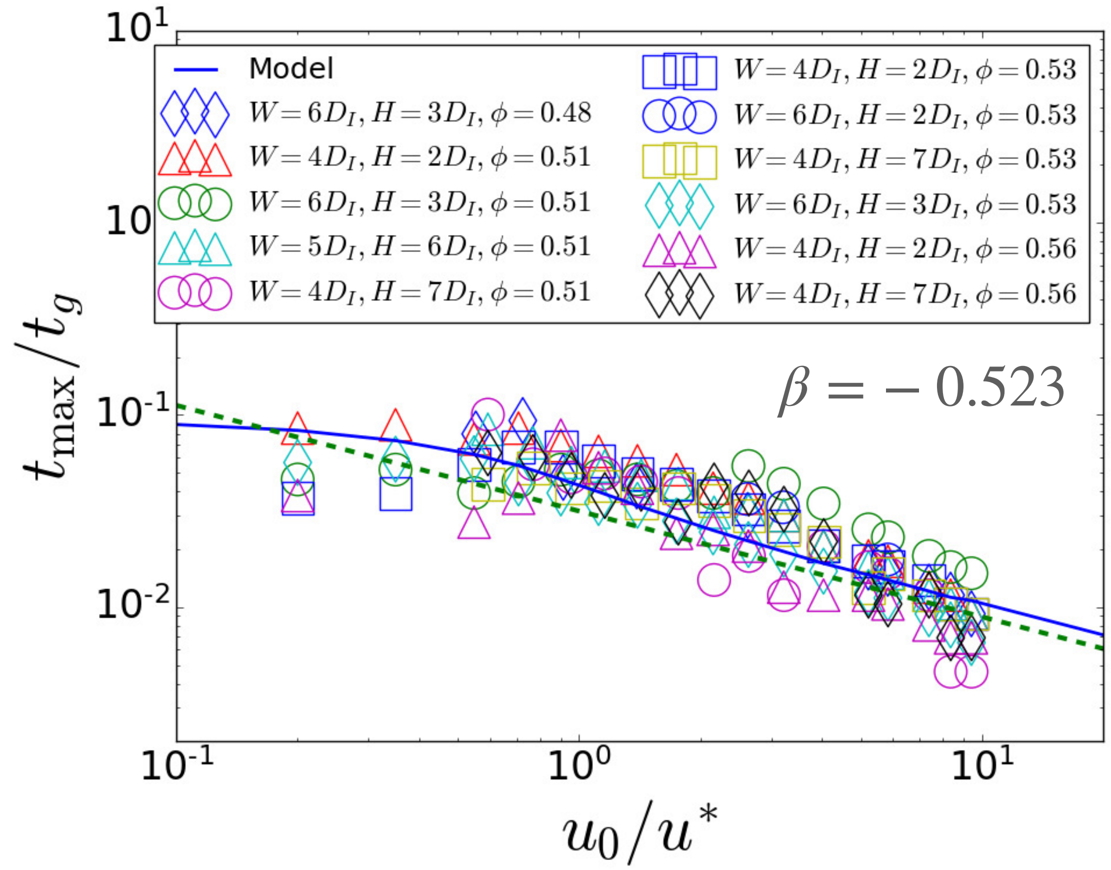

- **Crossover** from low u_0 to high u_0 regime
- Low u_0 regime: Independent of u_0
- High u_0 regime: $F_{\max} \propto u_0^{\alpha}$ and $t_{\max} \propto u_0^{\beta}$
- **Independent of system size**

Experiments:

$\alpha \approx 1.5 \quad t_{\max} \approx -0.5$

Brassard, et. al, **JFM** 923, A38 (2021)

How does this relationship connects with the rebound process?

Revisiting rebound process

Rebound depends on the depth of the container

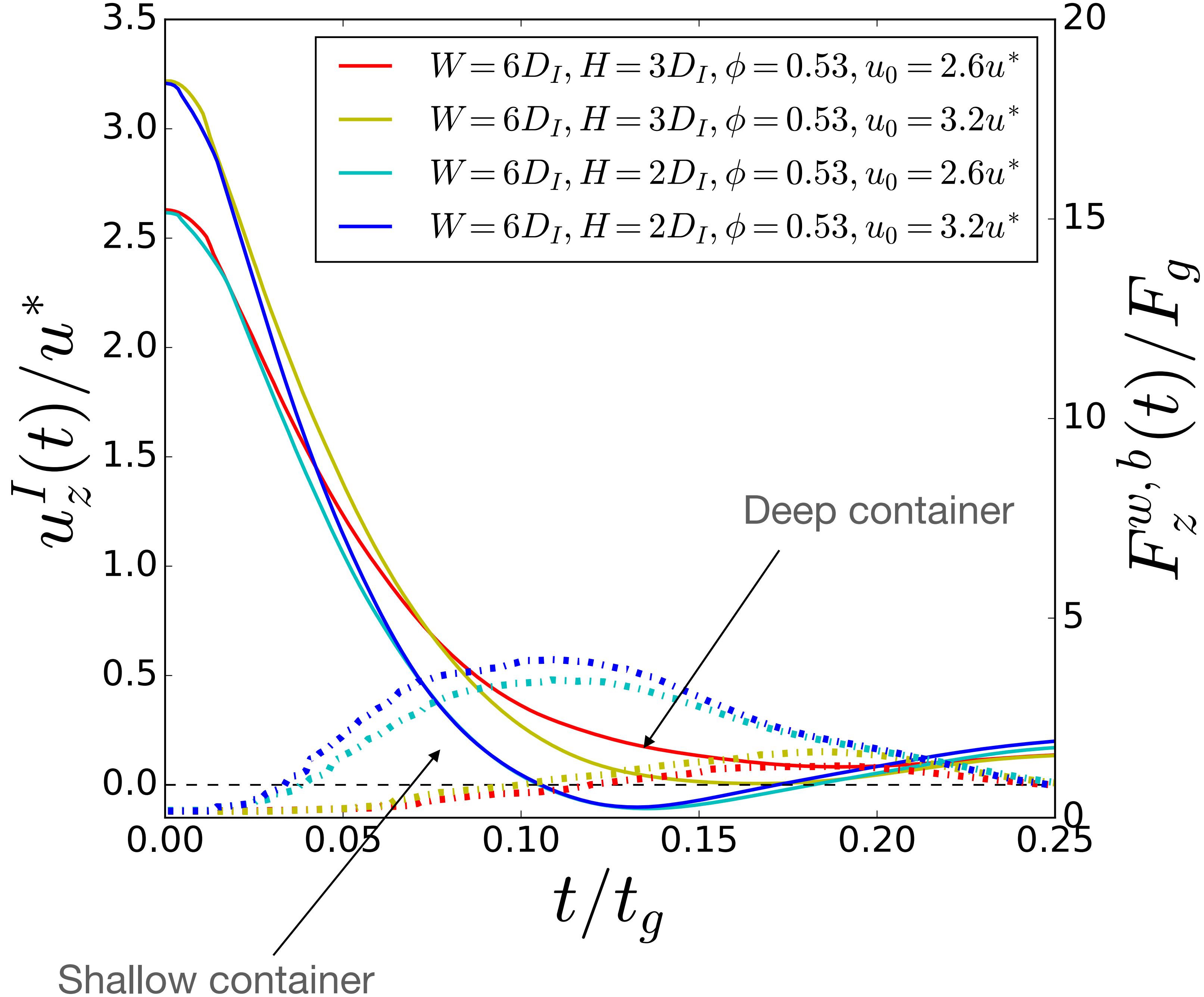

Force exerted on the bottom plate

Revisiting rebound process

Rebound and $t_{\max}$ takes place on different time

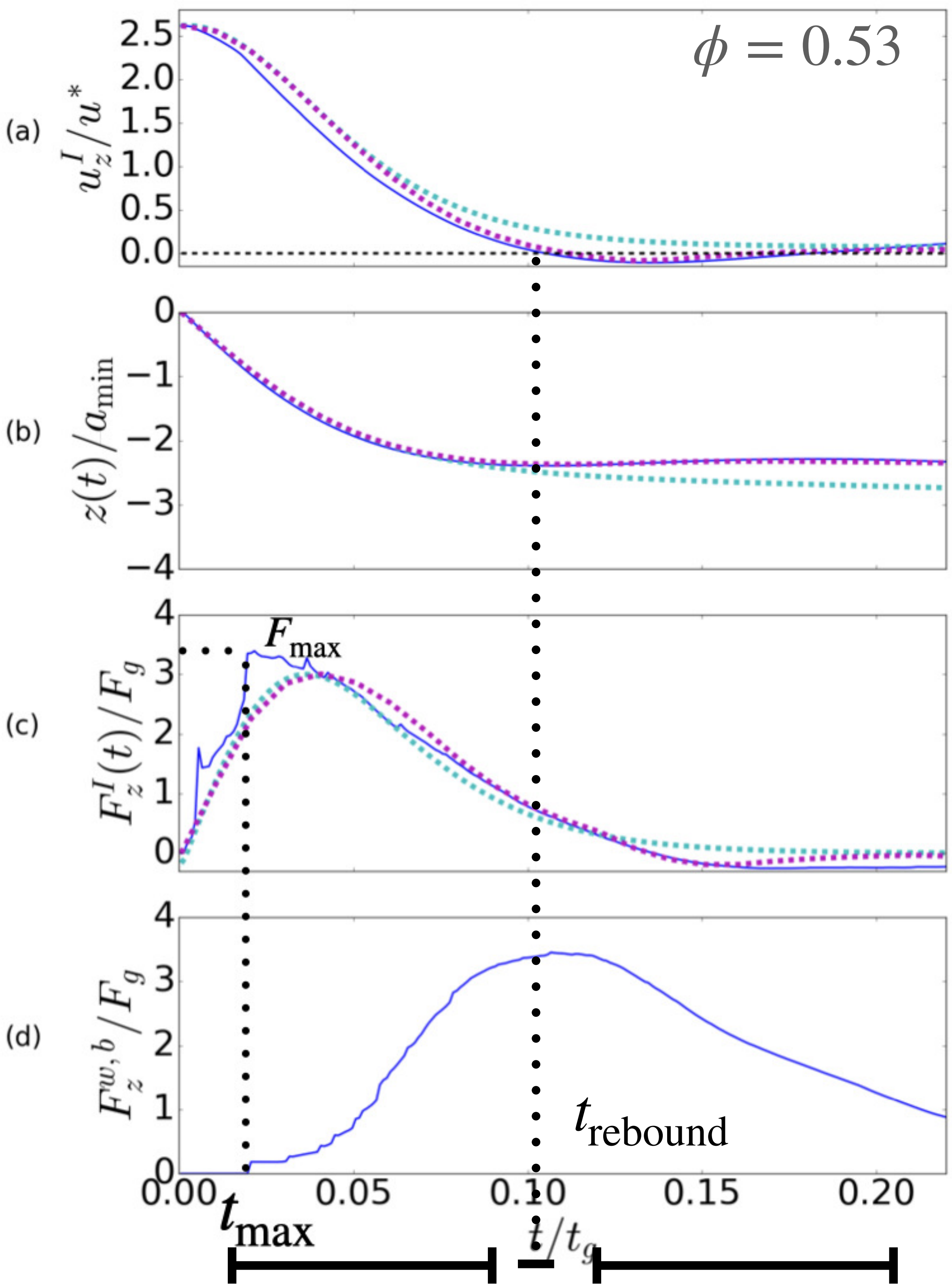

Dyn. jammed region touch the bottom and starts accumulating

Dyn. jammed region reached its peak on the bottom and soften → impactor starts to sink

The origin of $F_{\max}$ is the **floating** jammed region

The origin of rebound is the transmission of force from the impactor to the bottom plate and vice versa

Phenomenology *Floating model*

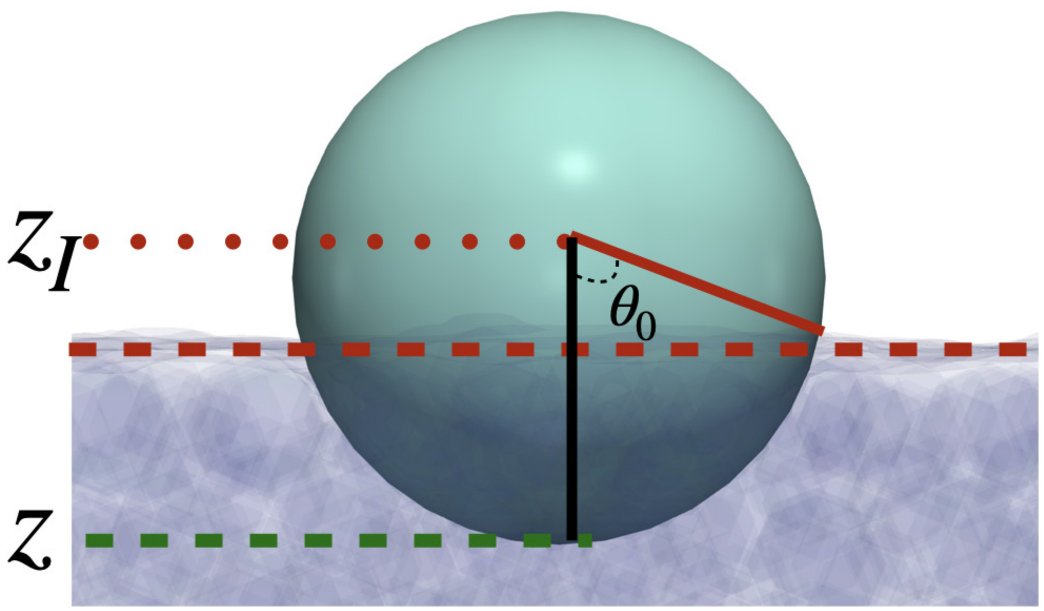

Drag on the impactor is proportional to its depth before completely immersed

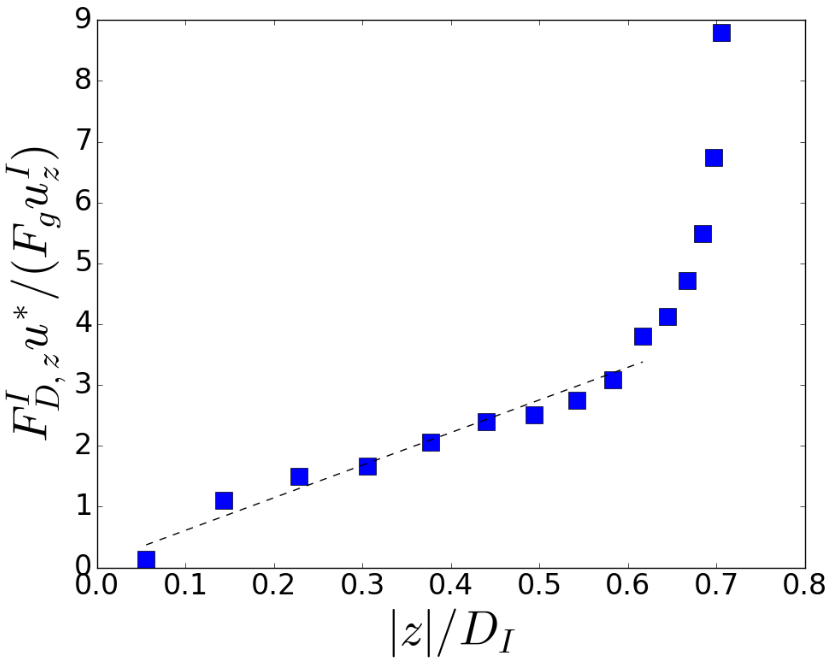

Stokes drag Pressure drag Friction drag

$$F^I_D = F^I_{D,p} + F^I_{D,f}$$

$$|z| = a_I(1 - \cos\theta_0)$$

$$F^I_D = 3\pi\eta_{\rm eff}\,\dot{z}_I\,|z|$$

For partially sinking sphere

$$F^I_{D,p} = 3\pi\eta_{\rm eff} a_I \dot{z}_I \int_0^{\theta_0} \cos^2\theta \sin\theta d\theta,$$

$$F^I_{D,f} = 3\pi\eta_{\rm eff} a_I \dot{z}_I \int_0^{\theta_0} \sin^3\theta d\theta$$

$$= 3\pi\eta_{\rm eff} a_I \dot{z}_I (1 - \cos\theta_0) - F^I_{D,p},$$

Drag term in floating model

$\eta_{\rm eff} \rightarrow$ Effective viscosity of the region beneath the impactor

Phenomenology *Capturing rebound*

The origin of the elastic rebound is the transmission of force from the impactor to the bottom plate and vice versa

Include elastic term to the model,

$$F_D^I = 3\pi\eta_{\mathrm{eff}} a_I \dot{z}_I |z| + n(t) k_n z_I$$

$k_n \rightarrow$ Spring constant of the DEM (particle's stiffness)

$n(t) \longrightarrow$ Numbers of percolating force chains from the impactor to the bottom boundary

Determining $n(t)$

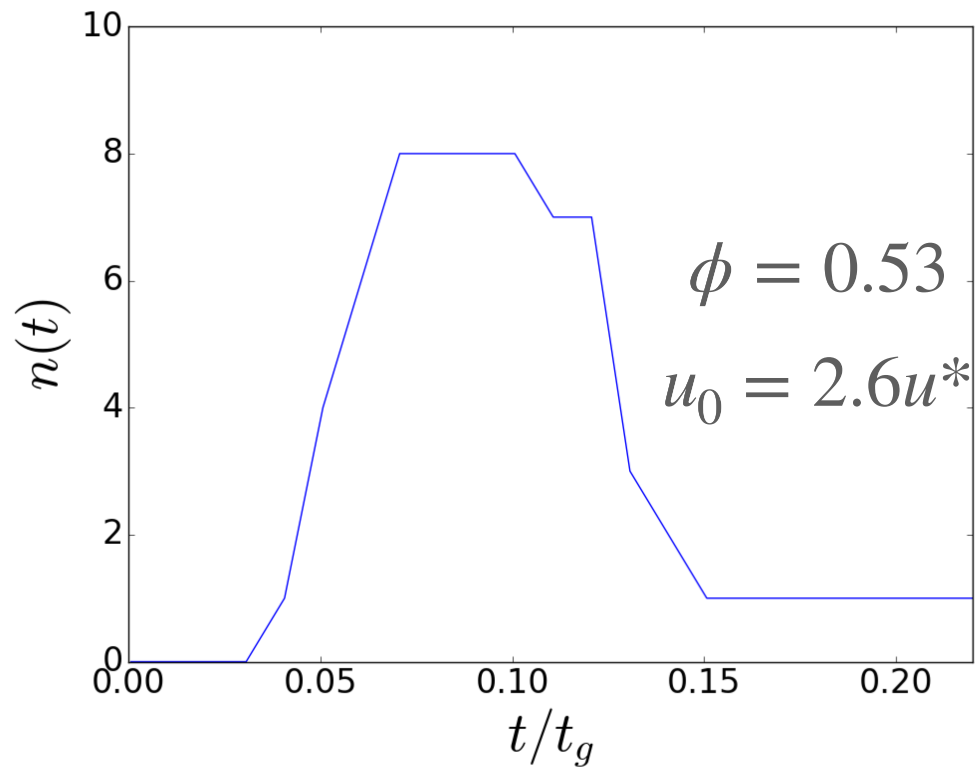

Phenomenology

$$m_I \frac{d^2 z_I}{dt^2} = \overset{\text{Gravity}}{- m_I \tilde{g}} + \overset{\text{Viscous (floating)}}{3\pi \eta_{\mathrm{eff}} \dot{z}_I |z|} + \overset{\text{Elastic}}{n(t) k_n z_I},$$

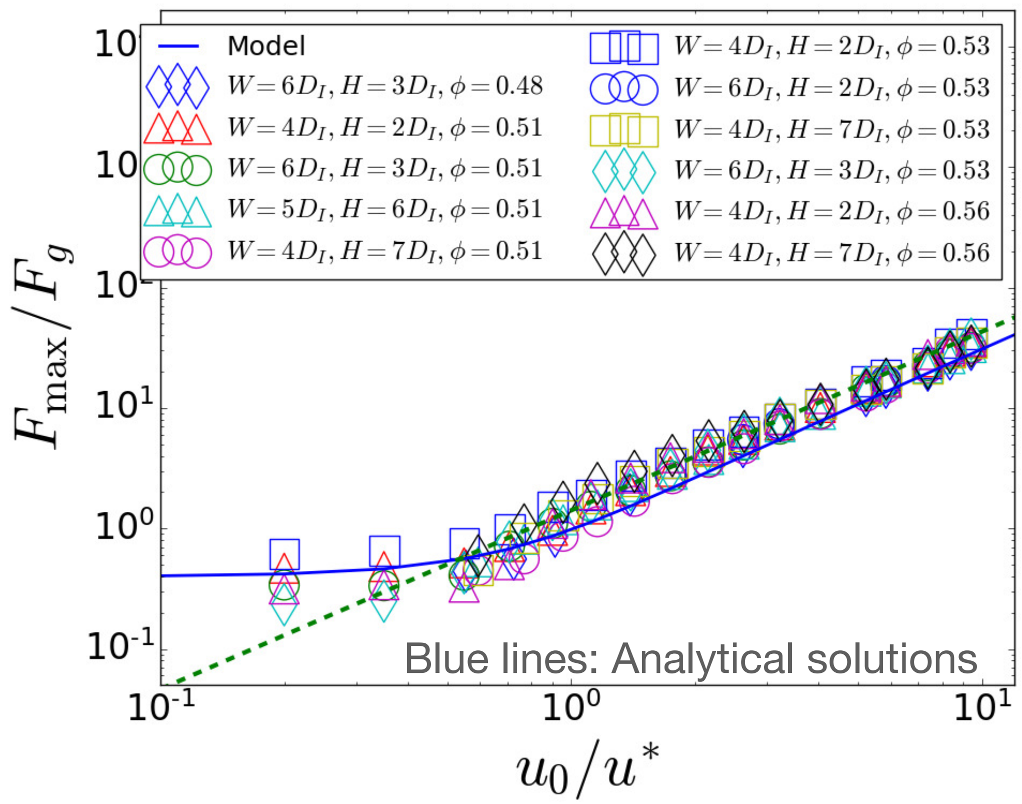

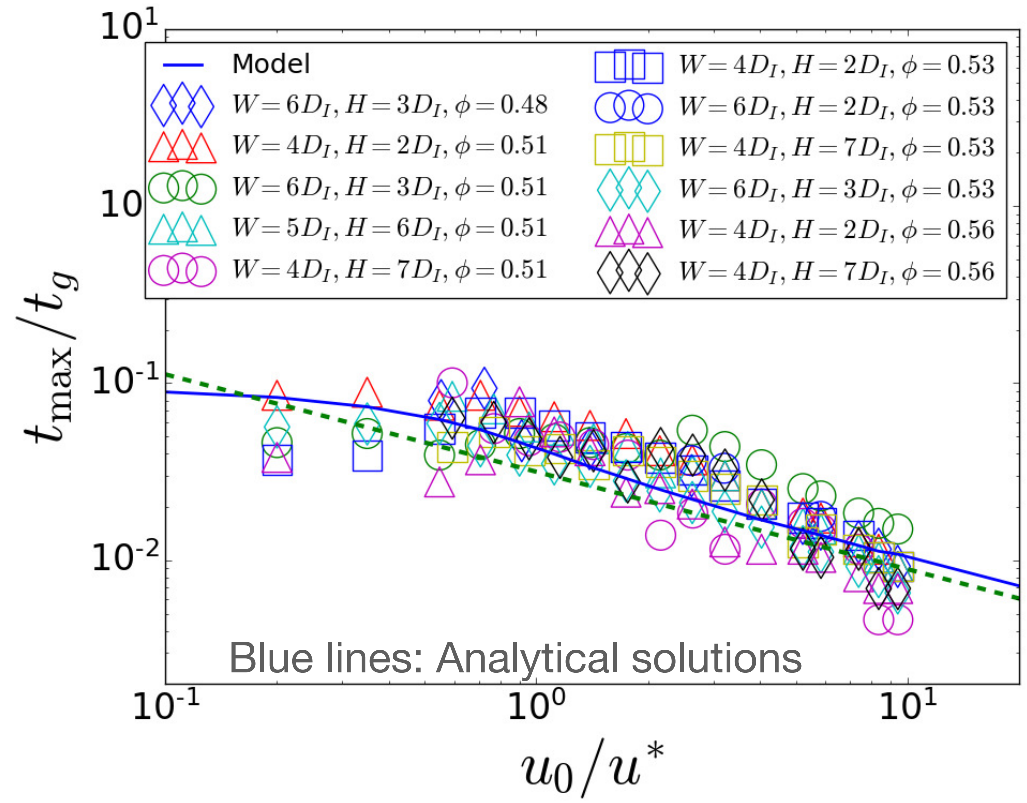

- Floating model can capture the crossover as well as the power-law exponent for high u_0
  - Floating model can be solved analytically
  - For $u_0 \gg 1/\eta_{\mathrm{eff}}$ one can obtain: $F_{\max} \propto u_0^{\frac{3}{2}}$ and $t_{\max} \propto u_0^{-\frac{1}{2}}$
- Elastic term from percolating force chains is necessary to recover rebound

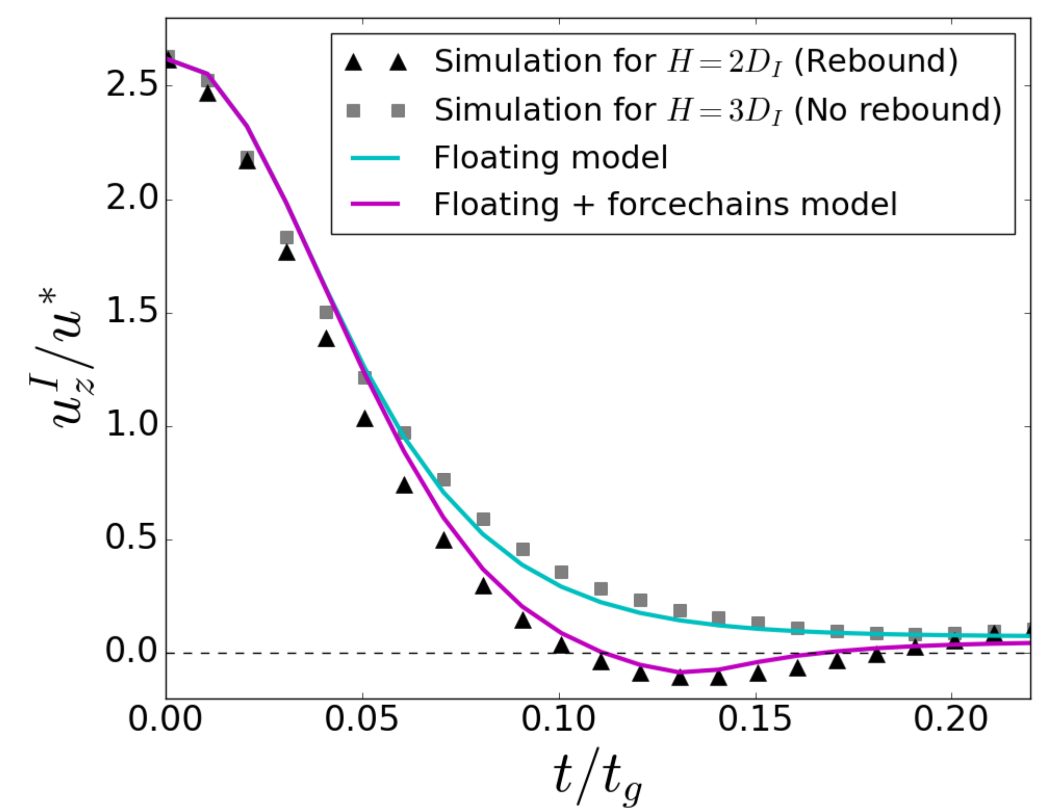

Discussions

Viscoelastic response of suspensions under impact

- F_{max} → viscous process
- Rebound → Elastic force from the the percolating force chains

The value of η_{eff} is about 100 times larger than the solvent viscosity and 5 times larger than the one observed in DST Pradipto and Hayakawa, Soft Matter **16**, 945 (2020)

- Viscosity enhancement of the dynamically jammed region

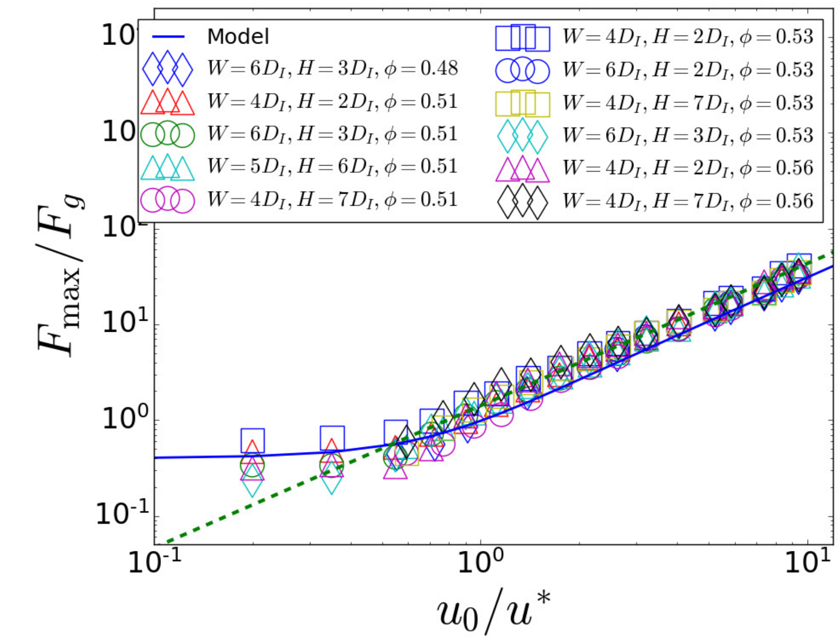

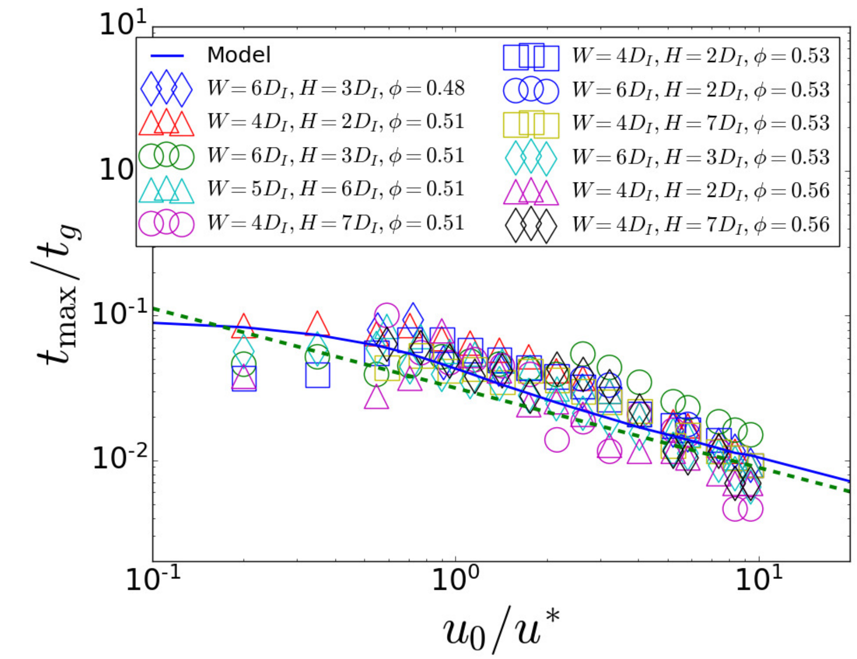

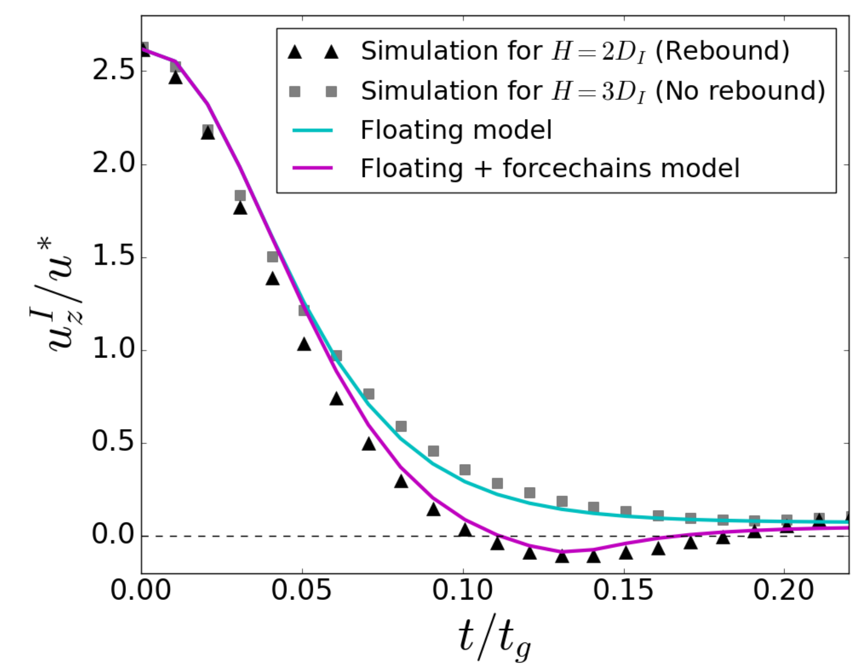

Conclusions

We found a crossover of $F_{\max}$ and $t_{\max}$ from low u_0 to high u_0 regime

For high u_0 regime: $F_{\max} \propto u_0^{1.432}$ and $t_{\max} \propto u_0^{-0.523}$, independent of system size

Rebound motion depends on the system size and takes place later than $t_{\max}$

Our phenomenology shows that $F_{\max}$ arises solely from the viscous process and rebound is originated from elastic force due to the percolating force chains